ehp ENVIRONMENTAL HEALTH PERSPECTIVES
http://www.ehponline.org

Erythrophagocytosis of Lead-Exposed Erythrocytes by Renal Tubular Cells: Possible Role in Lead-Induced Nephrotoxicity

So-Youn Kwon, Ok-Nam Bae, Ji-Yoon Noh, Keunyoung Kim, Seojin Kang, Young-Jun Shin, Kyung-Min Lim, and Jin-Ho Chung

http://dx.doi.org/10.1289/ehp.1408094

Received: 7 January 2014
Accepted: 7 October 2014
Advance Publication: 10 October 2014

Erythrophagocytosis of Lead-Exposed Erythrocytes by Renal Tubular Cells: Possible Role in Lead-Induced Nephrotoxicity

So-Youn Kwon,[1,*] Ok-Nam Bae,[2,*] Ji-Yoon Noh,[1] Keunyoung Kim,[1] Seojin Kang,[1] Young-Jun Shin,[2] Kyung-Min Lim,[3] and Jin-Ho Chung[1]

[1]College of Pharmacy, Seoul National University, Seoul, Korea; [2]College of Pharmacy, Hanyang University, Ansan, Korea; [3]College of Pharmacy, Ewha Womans University, Seoul, Korea.

[*]These authors contributed equally.

Address correspondence to Jin-Ho Chung, College of Pharmacy, Seoul National University, Seoul 151-742, Korea. Telephone: +82-2-880-7856. Fax: +82-2-885-4157. E-mail: jhc302@snu.ac.kr

Running title: Role of erythrocytes in lead-induced nephrotoxicity

Acknowledgments: This work was supported by the National Research Foundation of Korea (NRF) grant funded by the Korea Government (MSIP; No. 2007-0056817) and by a grant from Korea Food & Drug Administration in 2010.

Competing financial interests: None

Abstract

Background: Nephrotoxicity associated with lead poisoning has been frequently reported in epidemiological studies; but the underlying mechanisms have not been fully elucidated. **Objectives:** We examined the role of erythrocytes, one of the major lead reservoirs, in lead-associated nephrotoxicity.

Methods and results: Co-incubation of lead-exposed erythrocytes with renal proximal tubular cells (HK-2) resulted in renal tubular cytotoxicity, suggesting a role of erythrocytes in lead-induced nephrotoxicity. Morphological and flow cytometric analysis revealed that HK-2 actively phagocytized lead-exposed erythrocytes, which was associated with phosphatidylserine (PS) externalization on erythrocyte membrane and generation of PS-bearing microvesicles. Increased oxidative stress and up-regulation of nephrotoxic biomarkers such as NGAL were observed in HK-2 cells undergoing erythrophagocytosis. Moreover, TGF-β, a marker of fibrosis, was also significantly up-regulated. The significance of erythrophagocytosis in lead-induced nephrotoxicity was examined in rats exposed to lead via drinking water for 12 weeks. Iron deposition and generation of oxidative stress in renal tissues were observed in lead-exposed rats along with the histopathological alteration such as tubulointerstitial lesions, fibrosis and up-regulation of KIM-1, NGAL and TGF- β.

Conclusions: Our data strongly suggest that erythrophagocytosis and subsequent iron deposition in renal tubular cells could significantly enhance nephrotoxicity following lead exposure, shedding light on lead-associated kidney damages.

Introduction

Although environmental lead contamination has declined significantly since 1970s, lead exposure is still observed in children, industrial workers, and even in the general population (Hernberg, 2000). The average adult blood lead level (BLL) is 1-2 μg/dL and the Center for Disease Control (CDC) defines lead poisoning as BLL exceeding 10 μg/dL (0.5 μM) (CDC 1997). Epidemiological and toxicological studies revealed that lead induces toxicities on nervous, cardiovascular and renal systems (ASTDR 2007). Of these, the association between lead exposure and nephrotoxicity has been well-established, even in the population with BLL as low as 5 μg/dL (Ekong et al. 2006). Damage in kidney function is associated with albuminuria, reduced glomerular filtration rate and decreased creatinine clearance in lead-exposed populations (Fadrowski et al. 2010; Navas-Acien et al. 2009). Histopathologically, renal impairment associated with lead poisoning is characterized by the proximal tubular nephropathy, glomerular sclerosis and fibrosis in peritubular and interstitial lesion (Cramer et al. 1974; Diamond 2005; Goyer 1989; Loghman-Adham 1997).

Oxidative stress has been suggested to be the most convincing mechanism underlying lead-associated nephrotoxicity (Daggett et al. 1998; Wang et al. 2009). Pro-oxidant and antioxidant balance along with decreased glutathione and increased lipid peroxidation occurs in the kidney following lead exposure in animal models (Daggett et al. 1998; Liu et al. 2012; Patra et al. 2001; Wang et al. 2010). There have been several attempts to determine how lead increases oxidative stress in the kidney (Stacchiotti et al. 2009; Wang et al. 2009; Wang et al. 2011), but the exact mechanisms has not been clearly elucidated.

There is increasing evidence (Madsen et al. 1982; Mimura et al. 2008; Sheerin et al. 1999; Trump et al. 1969) that the kidney may play a role in the clearance of erythrocytes. Infiltration of erythrocytes was observed in proximal tubules and tubular lumen of renal biopsies from patients with acute glomerulonephritis and hematuria (Trump et al. 1969) or acute renal failure (Mimura et al. 2008). Iron deposition in the kidney was also found in the patients with various renal diseases (Wang et al. 2001), suggesting that the retention of iron-rich erythrocytes in the kidney may play a role in the pathogenesis of kidney diseases. The proximal tubular epithelial cells are capable of phagocytizing and degrading erythrocytes (Madsen et al. 1982; Sheerin et al. 1999), a phenomenon known as erythrophagocytosis. Erythrophagocytosis is primarily carried out by macrophages in the spleen and liver (Knutson and Wessling-Resnick 2003; Otogawa et al. 2007). Aged or damaged erythrocytes are phagocytized through erythrophagocytosis and cleared from systemic circulation. This process is mediated by externalized phosphatidylserine (PS) on outer membrane (Kobayashi et al. 2007; Mercer and Helenius 2008) and PS-bearing microvesicles (MV) (Knutson and Wessling-Resnick 2003; Otogawa et al. 2007). Although it has been reported that the proximal tubule cells can actively phagocytize erythrocytes in renal injury (Madsen et al. 1982; Sheerin et al. 1999), its toxicological significance in etiology of heavy metal-associated renal diseases remains to be established.

More than 99% of blood lead accumulates in erythrocytes, suggesting that erythrocytes may be a major target of systemic lead poisoning (Hernandez-Avila et al. 1998; Schutz et al. 1996). We recently demonstrated that lead significantly increases PS externalization in erythrocytes and enhances erythrophagocytosis by macrophages in spleen (Jang et al. 2011). Fowler *et al.* (1980) observed iron deposition in renal proximal tubule cells following administration of lead via

drinking water to rats, along with lead-associated histopathological lesions in the kidney. The present study examined the role of erythrocytes in lead-induced nephrotoxicity using *in vitro* co-culture system and *in vivo* in rats. Based on available evidence, we hypothesize that lead-induced PS externalization in erythrocytes promotes erythrophagocytosis in renal tubular cells, contributing to lead-associated kidney damage.

Materials and Methods

Chemicals

Lead(II) acetate, calcium chloride, glutaraldehyde solution, osmium tetroxide, bovine serum albumin (BSA), N-[2-hydroxyethyl]-piperazine-N-[2-ethanesulfonic acid] (HEPES), sodium citrate, dimethyl sulfoxide (DMSO), isopropanol, 3- (4,5-dimethylthiazol-2yl)-2,5-diphenyl-2H-tetrazolium bromide (MTT), dihyroethidium (DHE) were obtained from Sigma Chemical Co. (St Louis, MO). Phycoerythrin (PE)-labeled monoclonal antibody against human glycophorin A (anti-glycophorin A-RPE) was from Dako (Glostrub, Denmark) and fluo-4 acetoxymethyl ester (Fluo-4 AM) was from Molecular Probes (Eugene, OR). Fluorescein isothiocyanate (FITC)-labeled annexin V (annexin V-FITC) was from Pharmingen (San Diego, CA). 5-(-6)-Carboxyfluorescein diacetate (CFDA), calcein red-orange, anti-CD13-PE, anti-CD13-perCP-Cy5.5, and H2-DCFDA were obtained from Invitrogen (Eugene, OR). Keratinocyte serum free media kit was from Gibco BRL Life Technologies Inc. (Grand Island, NY). All other reagents were of the highest purity available.

Preparation of erythrocytes

With an approval from the Ethics Committee of Health Service Center at Seoul National University, human blood was obtained from Korean healthy male donors with informed consent

(N=20; aged 20-29 years) using a vacutainer with acid citrate dextrose and a 21-gauge needle (Becton Dickinson, Franklin Lakes, NJ) on the day of the experiment. Platelet rich plasma and buffy coat were removed by aspiration after centrifugation at 300 g for 15 min. Packed erythrocytes were washed three times with sterilized phosphate-buffered saline (PBS: 1 mM KH_2PO4, 154 mM NaCl, 3 mM Na_2HPO_4, pH 7.4) and once with filter-sterilized Ringer's solution (125 mM NaCl, 5 mM KCl, 1 mM $MgSO_4$, 32 mM HEPES, 5 mM glucose, pH 7.4). Washed erythrocytes were resuspended in Ringer's solution to a cell concentration of 5 x 10^7 cells/mL. $CaCl_2$ was added to erythrocytes as final concentration of 1 mM prior to use. The erythrocytes were used immediately after isolation without storage.

Cell culture

Renal proximal tubular cells, the cell population most susceptible to xenobiotic-induced toxicity in the kidney, were used. Human proximal tubular epithelial cell lines, HK-2, were purchased from the American Type Culture Collection (Manassas, VA) and maintained in keratinocyte serum free media supplemented with recombinant epidermal growth factor (rEGF), bovine pituitary extract (BPE), and 1% penicillin/streptomycin at 37°C under 5% CO_2 atmosphere (Ryan et al. 1994).

Measurement of cell viability

The cell viability was measured using MTT assay as previously described with slight modification (Thiebault et al. 2007). To evaluate the effect of Pb^{2+} on cell viability, HK-2 (2 x 10^5 cells per well in 6-well plate) were incubated with vehicle (1% distilled water, DW) or Pb^{2+} (10 or 20 μM) for 24 hr. MTT (0.5 mg/mL) was then incubated for 2 hr and washed, and the converted formazan was dissolved with 100% DMSO. The absorbance at 570 nm was measured

in a spectrophotometer (SpectraMax, Molecular Devices, Sunnyvale, CA). In experiments to examine the contribution of erythrocytes, vehicle or Pb^{2+} (10 or 20 μM) were added to erythrocytes for 1 hr and removed by centrifugation. HK-2 cells were co-incubated with Pb^{2+}-exposed erythrocytes (1 x 10^7 cells per well) for 24 hr. After co-incubation, erythrocytes were removed and MTT was added as described above.

Morphological examination

Erythrocytes were exposed to vehicle or Pb^{2+} (20 μM) for 1 hr and washed. HK-2 cells were co-incubated with vehicle- or Pb^{2+}-treated erythrocytes for 3 hr. Morphology was observed to measure the interaction between erythrocytes and HK-2 under phase contrast microscopy (Olympus IX70, Japan). For scanning electron microscopic observation (Jang et al. 2011; Noh et al. 2010), HK-2 cells co-incubated with vehicle- or Pb^{2+}-exposed erythrocytes were fixed with 2% glutaraldehyde for 1 hr at 4°C. Cells were washed three times with PBS and treated with 1% osmium tetroxide for 30 min at room temperature. After washing with PBS, the samples were dehydrated serially with 50, 70, 90, and 100% ethanol. After drying and coating with gold, the images were obtained on scanning electron microscope (JEOL, Tokyo, Japan).

Measurement of *in vitro* erythrophagocytosis

After treatment of vehicle or Pb^{2+} (10 or 20 μM) for 1 hr, erythrocytes were loaded with 10 μM CFDA for 30 min. HK-2 cells were co-incubated with vehicle- or Pb^{2+}-treated erythrocytes for 3 hr. After co-incubation, HK-2 cells were harvested and washed several times to remove remnant erythrocytes. Anti-CD13-PE was used to identify HK-2 cells. Samples were analyzed on the flow cytometer FACScalibur equipped with argon ion laser emitting at 488 nm (Becton Dickinson, Franklin Lakes, NJ). Cells were identified on the basis of their forward and side light

scatter characteristics (FSC and SSC, respectively), and the fluorescence signals from FL1 and FL2 were analyzed. Data from 10,000 events positive for PE (FL1) were collected and analyzed using CellQuest Pro software (Becton Dickinson). Cells with double positive signals for PE (FL1) and CFDA (FL2) were counted as HK-2 with erythrophagocytosis.

To investigate the role of externalized phosphatidylserine (PS) in erythrophagocytosis, purified annexin V (0.5 μM) that binds to the externalized PS and interrupts PS-mediated phenomena was used. Erythrocytes were incubated with purified annexin V for 2 min, and then exposed to lead for 1 hr. Erythrophagocytosis was measured as described above.

Analysis of phosphatidylserine exposure and microvesicle generation

Erythrocytes were exposed to vehicle or Pb^{2+} (10 or 20 μM) for 1 hr at 37°C, and incubated with annexin V-FITC, anti-glycophorin A antibody, and $CaCl_2$ (2.5 mM) for 30 min at room temperature in dark to detect PS externalization. Anti-glycophorin A antibody conjugated with PE was used as an identifier for erythrocytes and erythrocyte-derived microvesicles (MV). Isotype controls for measurement of non-specific annexin V binding were stained with annexin V-FITC in the presence of EDTA (2.5 mM) instead of $CaCl_2$. Samples were analyzed on the flow cytometer as described above.

***In vitro* ROS measurement**

Erythrocytes were loaded with 10 μM of calcein red-orange for 30 min after vehicle or Pb^{2+} (10 or 20 μM) was treated for 1 hr. HK-2 cells were loaded with H_2DCFDA for 30 min before co-incubation with vehicle- or Pb^{2+}-treated erythrocytes. After co-incubation for 4 hr, HK-2 cells were harvested and washed several times to remove excessive erythrocytes. Anti-CD13-perCP-

Cy5.5 was used to identify HK-2 cells. Samples were analyzed on the flow cytometer. As described above, HK-2 cells with erythrophagocytosis were determined as cells with double positive signals for perCP-Cy5.5 (FL3) and calcein red-orange (FL1). ROS generation was analyzed by DCF signal from the cells with erythrophagocytosis.

***In vitro* quantitative real time PCR**

After co-incubation with vehicle- or Pb^{2+} (10 or 20 μM)-exposed erythrocytes for 4 hr, total mRNA was isolated from HK-2 cells using Easy-Blue (Intron Biotechnology, Seongnam, Korea). Isolated mRNA was quantified spectrophotometrically in Nanodrop (Thermo Scientific, Wilmington, DE). cDNA was synthesized from isolated RNA using iScript™ (Bio-Rad, Hercules, CA). The levels of NGAL (neutrophil gelatinase-associated lipocalin) and KIM-1 (kidney injury molecule-1), the representative nephrotoxicity biomarkers, and TGF-β, an important mediator for renal fibrosis, were analyzed. Quantitative real-time PCR (qPT-PCR) was conducted using 2x SYBR green reaction buffer mixed with 0.5 μg cDNA and forward/reverse primers. Quantification of gene copies was carried on the CFX96™ Real-Time PCR Detection System (Bio-Rad), using iQ™ SYBR Green supermix (Bio-Rad). PCR cycles consisted of an initial step at 95ºC for 3 min followed by 45 cycles at 95ºC for 10 sec, 55ºC for 30 sec, and 72ºC for 10 sec. Relative mRNA expressions were calculated by the comparative CT method ($2^{-\Delta\Delta Ct}$), normalized to the endogenous 18S control. The specific primer sequences were as follows: h18S, forward: GTA ACC CGT TGA ACC CCA TT, reverse: CCA TCC AAT CGG TAG TAG CG; hKIM1, forward: GAA CAT AGT CTA CTG ACG GCC AAT AC, reverse: GAA CCT CCT TTT TGA AGA AAT ACT TTT T; hLCN2, forward: TCA CCT CCG TCC TGT TTA GG,

reverse: CGA AGT CAG CTC CTT GGT TC; hTGFB1, forward: CCC AGC ATC TGC AAA GCT C, reverse: GTC AAT GTA CAG CTG CCG CA.

In vivo animal treatment

All animal protocols were approved by the Ethics Committee of Animal Service Centre at Seoul National University, and the animals were treated humanely and with regard for alleviation of suffering. Male Sprague-Dawley rats (Samtako Co., Korea) weighing 200–250 g were used in all experiments. Before the experiments, animals were acclimated for 1 week in the laboratory animal facility maintained at constant temperature (22 ± 2ºC) and humidity (55 ± 5%) with a 12-hr light/dark cycle. Three rats were housed in one cage (W 260 x D 420 x H 180 mm). Food (Purinal Mills, Seongnam, Korea) and water were provided *ad libitum*. Lead was not assessed in food or untreated water, but blood lead levels in unexposed rats were below the detection limit (see Results.) We conducted our *in vivo* experiments in two independent trials, with rats randomly assigned to treatment groups. In the first trial, 4 rats were treated with 0 ppm and 4 were treated with 1000 ppm of lead-acetate containing drinking water for 12 weeks. Total mRNA was isolated from rat kidneys in a second trial in which 5, 6, or 5 rats were exposed to 0, 250, or 1000 ppm of lead-acetate containing drinking water for 12 weeks, respectively. The purity of one mRNA sample from the 250 ppm lead-exposed rats was not good enough for qRT-PCR, leaving 5 rats per treatment group. There was no significant difference between groups in body weight. The rats were euthanized by exsanguination from abdominal aorta under ether anesthesia. Animals were sacrificed at various times during the day, in a random sequence. Blood, spleen, kidney samples were collected, and further processed for biochemical analysis. The isolated kidney was blotted carefully and immediately weighed. Kidney was immediately

fixed or frozen for further histological examinations, isolation of mRNA and quantification of lead level. Spleen was fixed in 10% formalin for histological examination. Whole blood was used to isolated serum or immediately frozen for quantification of lead level. Serum was collected by centrifugation of blood and used to measure blood urea nitrogen (BUN) by enzymatic-kinetics method in Neodin Vetlab (Seoul, Korea). Lead level in frozen blood and kidney was analyzed with ICP-MS by National Center for Inter-University Research Facilities in Seoul National University (Seoul, Korea).

qRT-PCR from *in vivo* Pb^{2+}-treated kidney

Total mRNA was prepared from kidney samples isolated from lead-exposed rats. Frozen kidney tissue was homogenated in TRIzol (Life Technologies, Carlsbad, CA) and mRNA was further isolated with chloroform and isopropanol. Converting mRNA to cDNA and qRT-PCR were conducted as described above using iScript™ (Bio-Rad). Relative mRNA expressions for NGAL, KIM1, and TGF-β were calculated by the comparative CT method ($2^{-\Delta\Delta Ct}$), normalized to the endogenous 18S control. The specific primer sequences were as follows: r18S, forward: GTA ACC CGT TGA ACC CCA TT, reverse: CCA TCC AAT CGG TAG TAG CG; rKIM1, forward: GAA CAT AGT CTA CTG ACG GCC AAT AC, reverse: GAA CCT CCT TTT TGA AGA AAT ACT TTT T; rLCN2, forward: TCA CCT CCG TCC TGT TTA GG, reverse: CGA AGT CAG CTC CTT GGT TC; rTGFB1, forward: GGA CTA CTA CGC CAA AGA AG, reverse: TCA AAA GAC AGC CAC TCA GG.

Histological examination

To assess the histological damage, iron accumulation, ROS generation, and collagen accumulation, sections of kidney tissues were examined using staining with hematoxylin and

eosin (H&E), Prussian blue, dihydroethidium (DHE), and Masson trichrome, respectively. Formalin-fixed kidney tissues were used except DHE staining where optimum cutting temperature (OCT)-fixed frozen tissues were tested. Kidneys were fixed with 10% formalin, and the tissue specimens were cut into 4-μm thick sections and stained by H&E, Prussian blue, or Masson trichrome protocol by Reference Biolabs (Seoul, Korea). Formalin-fixed spleen tissues were handled in the same method by Prussian blue staining to measure iron accumulation. Slides were viewed with bright field microscope (Olympus CX41, Japan). Histopathological alteration was evaluated as focal nephropathy, glomerulonephropathy and tubulointerstitial lesion, which was scored by Prof. Byung-il Yoon (College of Veterinary Medicine, Kangwon National University, Korea). For ROS determination, kidney were frozen with OCT compound and cut into 4-μm thick sections and incubated in dihydroethidium (DHE) solution in dark for 30 min. Sections were washed with PBS and examined under fluorescence microscopes (Carl Zeiss Axiovert 200M, Germany).

Statistical analysis

The means and SEMs were calculated for all treatment groups. These data were subjected to one-way ANOVA followed by Duncan's multiple range test or Student's t-test to determine the statistical significance. In all cases, a p value of < 0.05 was considered significant.

Results

Lead (Pb^{2+})-induced erythrophagocytosis by renal tubular epithelial cells

In order to examine the role of erythrocytes (red blood cells; RBC) in lead-associated kidney injury, co-incubation system of erythrocyte-tubular cell (HK-2) was employed. Freshly isolated human erythrocytes were exposed to Pb^{2+} (lead acetate; 0, 10 or 20 μM) for 1 hr, and then added

to renal tubular cells. As shown in Figure 1A, co-incubation of Pb^{2+}-exposed erythrocytes with HK-2 for 24 hr significantly reduced HK-2 cell viability while Pb^{2+} alone failed to affect HK-2 viability, supporting a central role of erythrocytes in Pb^{2+}-induced HK-2 cytotoxicity. In microscopic examination, adherence of Pb^{2+}-exposed erythrocytes to HK-2 was observed, while untreated discocytic erythrocytes did not bind to HK-2 cells (Figure 1B). Images from scanning electron microscopy further confirmed the interaction between HK-2 and Pb^{2+}-exposed spherocytic erythrocytes, along with the roughening of HK-2 membrane (Figure 1C). Next, we investigated if Pb^{2+} could enhance erythrophagocytosis by HK-2 using flow cytometric analysis. The extent of phagocytosis, as determined by the number of HK-2 cells positive of the erythrocyte marker, was significantly increased by Pb^{2+} exposure ($p<0.01$; Figure 1D).

Role of Pb^{2+}-induced erythrophagocytosis in renal tubular damage

Previous studies have shown that erythrophagocytosis by macrophage is mediated by phosphatidylserine (PS) exposed on outer membrane of erythrocytes (Jang et al. 2011; Noh et al. 2010). To clarify if Pb^{2+}-induced PS externalization may contribute to erythrophagocytosis by renal tubular cells, we examined PS externalization in erythrocytes following Pb^{2+} treatment. The binding of annexin V, a marker for exposed PS, was increased in Pb^{2+}-treated erythrocytes (Figure 2A), and the generation of PS-bearing microvesicles (MVs) was also enhanced by Pb^{2+} (Figure 2B). Notably, when the exposed PS was neutralized by exogenously added annexin V, Pb^{2+}-induced erythrophagocytosis was significantly inhibited, suggesting that PS externalized on erythrocytes plays a key role in erythrophagocytosis by renal tubular cells (Figure 2C).

Next we evaluated the potential role of erythrophagocytosis in renal tubular damage. Considering that erythrocytes contain high amount of iron which can accumulate and induce

excessive oxidative stress (Zager et al. 2002), we measured the generation of reactive oxygen species (ROS) in HK-2 cells. Co-incubation of Pb^{2+}-exposed erythrocytes increased ROS generation in HK-2 cells, reflecting that Pb^{2+}-induced erythrophagocytosis resulted in oxidative stress (Figure 2D). We also evaluated tubular damage by measuring mRNA level of NGAL (neutrophil gelatinase-associated lipocalin) and KIM-1 (kidney injury molecule-1), the representative nephrotoxicity biomarkers (Figure 2E). The mRNA expression of NGAL in HK-2 was significantly increased by Pb^{2+}-enhanced erythrophagocytosis, and there was a certain trend of increased KIM-1 expression although statistical significance was not achieved (p=0.11).

In vivo erythrophagocytosis in the kidney following Pb^{2+} exposure

To evaluate *in vivo* relevancy of our finding, we investigated the contribution of erythrophagocytosis in Pb^{2+}-associated nephrotoxicity *in vivo*. Following exposure of rats to lead (II) acetate-containing drinking water for 12 weeks (0, 250, and 1,000 ppm Pb^{2+}), kidney, spleen and blood were isolated for biochemical and histological analysis. Blood lead levels in rats exposed to lead-containing drinking water were 2.11 ± 0.54 μM (250 ppm Pb^{2+}) and 3.53 ± 0.84 μM (1000 ppm Pb^{2+}), while the levels of blood lead in control rats were below detection limit. The lead levels in kidney samples were 0.08 ± 0.05 μg/g, 12.29 ± 4.63 μg/g, and 26.67 ± 3.67 μg/g for 0, 250, and 1000 ppm Pb^{2+}-exposed rats, respectively. Pb^{2+} exposure increased iron accumulation in spleen (Figure 3A), which matched well our previous report (Jang et al. 2011). We could observe iron accumulation in the kidney (Figure 3B). Generation of ROS was found in kidney tissue from Pb^{2+}-treated rats (Figure 4A).

Evaluation of renal damage associated with Pb^{2+}-exposure

Along with iron accumulation and ROS generation in the kidney, we evaluated if Pb^{2+} treatment induced kidney damage. Histopathological examination revealed Pb^{2+}-induced morphological alteration such as tubulointerstitial lesions characterized by basophilic regenerating tubules with altered morphology of epithelial cells, and interstitial lymphotic cell infiltration (Figure 4B). Conventional nephrotoxicity markers such as the relative kidney weights and serum BUN, were markedly increased by Pb^{2+} treatment, but statistical significance was not obtained (Figure 4C and D). Meanwhile, the mRNA levels of nephrotoxic biomarkers (KIM-1 and NGAL) were significantly increased by Pb2+ treatment (Figure 4E), supporting Pb^{2+}-induced kidney damage.

It is known that chronic exposure to Pb^{2+} is associated with renal fibrosis (Cramer et al. 1974), which could ultimately disrupt normal kidney function. To evaluate the role of erythrophagocytosis in Pb^{2+}-associated renal fibrosis, we examined the collagen accumulation as well as the induction of TGF-β, an important mediator for renal fibrosis. Exposure to Pb^{2+}-containing drinking water increased collagen deposition and TGF-β mRNA expression in the kidney (Figure 5A and 5B). Notably, the expression of TGF-β was also significantly increased in HK-2 by co-incubation of Pb^{2+}-exposed erythrocytes (Figure 5C), demonstrating that Pb^{2+}-associated erythrophagocytosis may play important roles in Pb^{2+}-associated renal fibrosis.

Discussion

Here we demonstrated that erythrocytes may play an important role in the potentiation of lead (Pb^{2+}) -induced nephrotoxicity through PS-mediated erythrophagocytosis. While the treatment of Pb^{2+} alone failed to induce statistically significant cytotoxicity to HK-2 renal tubular cells up to 20 μM, co-incubation of erythrocytes exposed to Pb^{2+} significantly decreased cell viability at as

low as 10 μM. Increased oxidative stress and up-regulation of nephrotoxic biomarkers such as NGAL were also observed in HK-2 cells co-incubated with lead-exposed erythrocytes. Moreover, TGF- β, a marker of fibrosis was significantly up-regulated. The role of erythrocytes in lead-induced nephrotoxicity was also confirmed *in vivo* in rats exposed to lead via drinking water for 12 weeks as determined by increased iron deposition and generation of oxidative stress in renal tissues along with fibrosis and expression of KIM-1, NGAL and TGF-β.

Lead contamination is a significant environmental threat to public health. Among the lead-associated adverse health effects, nephrotoxicity as represented by proximal tubular nephropathy and interstitial fibrosis has been frequently reported in epidemiological studies (Cramer et al. 1974; Navas-Acien et al. 2009). High BLL (70-80 μg/dL) is known to be an established risk factor for chronic renal damage (Ekong et al. 2006; Fadrowski et al. 2010). Despite the robust epidemiological evidence, the mechanisms underlying lead-induced nephrotoxicity have not been fully understood. Especially, *in vitro* studies employing renal cells revealed that kidney cells were somewhat resistant to lead-induced cytotoxicity as our results, and higher concentrations of lead than the reported BLLs in human were required to manifest oxidative stress and cytotoxicity (Stacchiotti et al. 2009). Here we demonstrated that erythrophagocytosis by kidney cells may underlie the lead-induced nephrotoxicity cytotoxicity, providing an important clue to explain the discrepancy. Although we might not completely exclude the possibility of direct effects of lead on the kidney after chronic exposure *in vivo*, our data strongly suggest that erythrophagocytosis and subsequent iron deposition could contribute to lead-associated kidney damage. Experiments are needed to determine if blockage or neutralization of

the externalization of PS or attenuation of iron-mediated ROS generation could reverse lead-associated nephrotoxicity.

Heavy metals that are absorbed into bloodstream, are continuously exposed to and accumulated into erythrocytes. In case of lead, it is known that 99% of blood lead is associated with erythrocytes (Hernandez-Avila et al. 1998; Schutz et al. 1996). Lead induced disruption of membrane-lipid asymmetry and subsequent phosphatidylserine (PS) externalization in erythrocytes, which is mediated by alteration of aminophospholipid translocase activities (Jang et al. 2011; Kempe et al. 2005) and activation of transbilayer lipid movement (Shettihalli and Gummadi 2013). Externalization of PS by lead treatment can induce erythrophagocytosis by interacting with scavenger receptors on macrophages in spleen (Willekens et al. 2005). PS-exposing erythrocytes can be also engulfed by other tissue that can eventually cause certain pathogenic effects (Fens et al. 2012; Otogawa et al. 2007). Otogawa *et al.* (2007) showed that high fat diet induced PS externalization on erythrocytes and erythrophagocytosis by Kupffer cells in the liver, resulting in inflammation and hepatic fibrosis. Fens *et al.* (2012) demonstrated that activated endothelial cells were capable of erythrophagocytosis, leading to endothelial cytotoxicity. Ichimura *et al.* (2008) showed that KIM-1 in kidney tubular epithelial cells specifically recognizes PS, and is responsible for phagocytosis. Loss of phospholipid asymmetry in erythrocytes was also observed in uremia (Kong et al. 2001) and chronic renal failure (Bonomini et al. 1999; Bonomini et al. 2001). While erythrophagocytosis by renal tubular cells has been confirmed in several reports (Madsen et al. 1982; Mimura et al. 2008), its pathophysiological significance has not been elucidated. The results in our study showed that lead-induced erythrophagocytosis was associated with increased oxidative stress and histological

changes in renal cells. Additional research is needed to examine the potential role that erythrophagocytosis may play in the pathogenesis of kidney disease.

In addition to the transport of lead accumulated in erythrocytes to the kidney, the pathological role of erythrophagocytosis may stem from iron abundance in erythrocytes. Erythrocytes contain about 70 percent of the body iron content by the form of hemoglobin, and abnormal uptake of damaged erythrocytes by intact tissues can result in iron accumulation and subsequent cellular damages. Iron overload stimulates ROS generation by oxidation-reduction reaction (Fraga and Oteiza 2002; Valko et al. 2005). Deposition of large amounts of free iron is known to cause critical damage in the liver, the heart and other organs (Rasmussen et al. 2001). In the kidney, ROS-mediated lipid peroxidation (Zager et al. 2002) and renal fibrosis (Kovtunovych et al. 2010) can be induced by iron accumulation, ultimately leading to tubular cytotoxicity (Zager et al. 2004). Our study suggests that erythrophagocytosis may explain the potential source of iron accumulation and ROS generation in the kidneys following lead-exposure.

The average BLL in adult is reported to be 1-2 μg/dL (approximately 0.05-0.1 μM) while BLL exceeding 10 μg/dL (0.48 μM) is defined as lead poisoning (CDC 1997). Lead exposure-associated nephrotoxicity has been observed at BLL as low as 5 μg/dL (Ekong et al. 2006), and BLL is a known risk factor for nephropathy (Muntner et al. 2003). During 2002-2011, ABLES (Adult Blood Lead Epidemiology and Surveillance) program from CDC identified 11,536 adults with very high BLLs (≥ 40 μg/dL), and 19% of these adults with persistent very high BLLs (≥ 40 μg/dL in ≥ 1 calendar year) in US, showing that lead exposures continue to occur at unacceptable levels. In rat models, histological and functional damages in kidney became evident at BLL of 36-72 μg/dL (Mahaffey et al. 1980, Liu et al. 2012). To achieve high BLL for the study on the

mechanism underlying lead-associated nephrotoxicity, we exposed rats to 1,000 ppm Pb^{2+} in drinking water (mean BLL was 73.5 ± 17.4 μg/dL and the lead levels in the kidney tissue was 26.67 ± 3.67 μg/g in the lead-exposed rats). While achieved BLL was epidemiologically reasonable, lead level in drinking water may appear rather high; however, considering that 80% of environmental lead exposure is from other sources like food or inhalation other than drinking water, adoption of this high lead levels in drinking water was necessary in our experimental system where drinking water is an absolute source of lead-exposure.

In our *in vitro* experiments, we demonstrated that co-incubation of erythrocytes exposed to Pb^{2+} at concentration ranges up to 20 μM for 1 hr with HK-2 cells induced erythrophagocytosis and subsequent cytotoxicity. Although we could not extend the duration of Pb^{2+} exposure beyond 1 hr in our experimental setting due to technical limitation to maintain erythrocyte integrity for 24 hr co-incubation, we believe that prolonged exposure to lower concentration of Pb^{2+} could affect renal tubular viability through PS-exposure mediated erythrophagocytosis. In our previous study, we demonstrated that similar level of PS externalization obtained by Pb^{2+} 20 μM with 1 hr, was induced by Pb^{2+} 0.5 μM with 24 hr incubation (Jang et al. 2011), suggesting that erythrophagocytosis can be induced at much lower concentration of Pb^{2+} when exposed chronically as observed in real-life scenario.

Erythrocyte uptake in kidney induced iron deposition, ROS generation and renal fibrosis. Fibrosis is a major determinant of progressive renal damage leading to end-stage renal failure (Eddy 1996), and has been frequently observed in lead-exposed population (ASTDR 2007). We found typical characteristics of tubulointerstitial fibrosis, such as tubular loss and accumulation of collagen, the most abundant protein in the extracellular matrix (ECM) proteins, in lead-

exposed rat kidneys. It is known that ECM is primarily produced by myofibroblasts (LeBleu et al. 2013); however, the active role of tubular epithelial cells in fibrosis is also reported. In pathological states such as diabetes and hypertension, the potent profibrotic cytokine TGF-β (Isaka et al. 2000) is produced by tubular cells, and stimulates renal fibroblast to produce ECM (Vallon and Thomson 2012; Zhao et al. 2008). TGF-β also induces fibrogenic trans-differentiation of tubular epithelial cells to harbor ECM producing character (Li et al. 2002). TGF-β expression in tubular cells could be induced by excessive oxidative stress (Vallon and Thomson 2012; Zhao et al. 2008). We have shown the ROS generation and TGF-β up-regulation in the kidney of lead-exposed rats *in vivo* and tubular cells undergoing erythrophagocytosis *in vitro*, suggesting the potential contribution of lead-induced erythrophagocytosis to renal fibrosis. These findings matched well a previous study demonstrating the up-regulation of NGAL and KIM-1 in tubular cells as key renal injury biomarkers (Lock 2010).

Conclusion

The results of our studies suggest that exposure to lead can lead to the externalization of PS and generation of MV in erythrocytes, which appears to be associated with increased erythrophagocytosis in renal tubular cells. Our data supports the hypothesis that erythrophagocytosis seems to be associated with increased ROS generation, induction of nephrotoxicity biomarkers, TGF-β up-regulation, and decreased cell viability of renal tubular cells. Our *in vivo* experiments confirmed that chronic exposure to lead increases iron deposition in the kidney. The role that iron plays in lead-mediated oxidative stress and renal fibrosis warrants further research. We believe that our study gives a new insight into the mechanisms of lead exposure-associated nephrotoxicity.

References

ASTDR. 2007. Toxicological profile for lead. Atlanta, GA:Agency for Toxic Substances and Disease Registry.

Bonomini M, Sirolli V, Settefrati N, Dottori S, Di Liberato L, Arduini A. 1999. Increased erythrocyte phosphatidylserine exposure in chronic renal failure. J Am Soc Nephrol 10:1982-1990.

Bonomini M, Sirolli V, Reale M, Arduini A. 2001. Involvement of phosphatidylserine exposure in the recognition and phagocytosis of uremic erythrocytes. Am J Kidney Dis 37:807-814.

CDC. 1997. Screening young children for lead poisoning: Guidance for state and local public health officials. Atlanta, GA:Centers for Disease Control and Prevention.

CDC. 2013. Very high blood lead levels among adults - United States, 2002-2011. MMWR Morb Mortal Wkly Rep. 62:967-971.

Cramer K, Goyer RA, Jagenburg R, Wilson MH. 1974. Renal ultrastructure, renal function, and parameters of lead toxicity in workers with different periods of lead exposure. Br J Ind Med 31:113-127.

Daggett DA, Oberley TD, Nelson SA, Wright LS, Kornguth SE, Siegel FL. 1998. Effects of lead on rat kidney and liver: Gst expression and oxidative stress. Toxicology 128:191-206.

Diamond GL. 2005. Risk assessment of nephrotoxic metals. In: The toxicology of the kidney, (Tarloff J, Lash L, eds). London:CRC Press, 1099-1132.

Eddy AA. 1996. Molecular insights into renal interstitial fibrosis. J Am Soc Nephrol 7:2495-2508.

Ekong EB, Jaar BG, Weaver VM. 2006. Lead-related nephrotoxicity: A review of the epidemiologic evidence. Kidney Int 70:2074-2084.

Fadrowski JJ, Navas-Acien A, Tellez-Plaza M, Guallar E, Weaver VM, Furth SL. 2010. Blood lead level and kidney function in us adolescents: The third national health and nutrition examination survey. Arch Intern Med 170:75-82.

Fens MH, van Wijk R, Andringa G, van Rooijen KL, Dijstelbloem HM, Rasmussen JT, et al. 2012. A role for activated endothelial cells in red blood cell clearance: Implications for vasopathology. Haematologica 97:500-508.

Fowler BA, Kimmel CA, Woods JS, McConnell EE, Grant LD. 1980. Chronic low-level lead toxicity in the rat. Iii. An integrated assessment of long-term toxicity with special reference to the kidney. Toxicol Appl Pharmacol 56:59-77.

Fraga CG, Oteiza PI. 2002. Iron toxicity and antioxidant nutrients. Toxicology 180:23-32.

Goyer RA. 1989. Mechanisms of lead and cadmium nephrotoxicity. Toxicol Lett 46:153-162.

Hernandez-Avila M, Smith D, Meneses F, Sanin LH, Hu H. 1998. The influence of bone and blood lead on plasma lead levels in environmentally exposed adults. Environ Health Perspect 106:473-477.

Hernberg S, 2000. Lead poisoning in a historical perspective. Am J Ind Med 38: 244–254.

Ichimura T, Asseldonk EJ, Humphreys BD, Gunaratnam L, Duffield JS, Bonventre JV. 2008. Kidney injury molecule-1 is a phosphatidylserine receptor that confers a phagocytic phenotype on epithelial cells. J Clin Invest 118:1657-1668.

Isaka Y, Tsujie M, Ando Y, Nakamura H, Kaneda Y, Imai E, et al. 2000. Transforming growth factor-beta 1 antisense oligodeoxynucleotides block interstitial fibrosis in unilateral ureteral obstruction. Kidney Int 58:1885-1892.

Jang WH, Lim KM, Kim K, Noh JY, Kang S, Chang YK, et al. 2011. Low level of lead can induce phosphatidylserine exposure and erythrophagocytosis: A new mechanism underlying lead-associated anemia. Toxicol Sci 122:177-184.

Kempe DS, Lang PA, Eisele K, Klarl BA, Wieder T, Huber SM, et al. 2005. Stimulation of erythrocyte phosphatidylserine exposure by lead ions. Am J Physiol Cell Physiol 288:C396-402.

Knutson M, Wessling-Resnick M. 2003. Iron metabolism in the reticuloendothelial system. Crit Rev Biochem Mol Biol 38:61-88.

Kobayashi N, Karisola P, Pena-Cruz V, Dorfman DM, Jinushi M, Umetsu SE, et al. 2007. Tim-1 and tim-4 glycoproteins bind phosphatidylserine and mediate uptake of apoptotic cells. Immunity 27:927-940.

Kong QY, Wu X, Li J, Peng WX, Ye R, Lindholm B, et al. 2001. Loss of phospholipids asymmetry in red blood cells contributes to anemia in uremic patients. Adv Perit Dial 17:58-60.

Kovtunovych G, Eckhaus MA, Ghosh MC, Ollivierre-Wilson H, Rouault TA. 2010. Dysfunction of the heme recycling system in heme oxygenase 1-deficient mice: Effects on macrophage viability and tissue iron distribution. Blood 116:6054-6062.

LeBleu VS, Taduri G, O'Connell J, Teng Y, Cooke VG, Woda C, Sugimoto H, Kalluri R. 2013. Origin and function of myofibroblasts in kidney fibrosis. Nat Med 19:1047-1053.

Li JH, Zhu HJ, Huang XR, Lai KN, Johnson RJ, Lan HY. 2002. Smad7 inhibits fibrotic effect of tgf-beta on renal tubular epithelial cells by blocking smad2 activation. J Am Soc Nephrol 13:1464-1472.

Liu CM, Ma JQ, Sun YZ. 2012. Puerarin protects rat kidney from lead-induced apoptosis by modulating the PI3K/Akt/eNOS pathway. Toxicol Appl Pharmacol 258:330-342.

Liu CM, Sun YZ, Sun JM, Ma JQ, Cheng C. 2012. Protective role of quercetin against lead-induced inflammatory response in rat kidney through the ros-mediated mapks and nf-kappab pathway. Biochim Biophys Acta 1820:1693-1703.

Lock EA. 2010. Sensitive and early markers of renal injury: Where are we and what is the way forward? Toxicol Sci 116:1-4.

Loghman-Adham M. 1997. Renal effects of environmental and occupational lead exposure. Environ Health Perspect 105:928-938.

Madsen KM, Applegate CW, Tisher CC. 1982. Phagocytosis of erythrocytes by the proximal tubule of the rat kidney. Cell Tissue Res 226:363-374.Mahaffey KR, Rader JI, Schaefer JM, Kramer SN. 1980. Comparative toxicity to rats of lead acetate from food or water. Bull Environ Contam Toxicol 25:541-546.

Mercer J, Helenius A. 2008. Vaccinia virus uses macropinocytosis and apoptotic mimicry to enter host cells. Science 320:531-535.

Mimura I, Tojo A, Uozaki H, Fujita T. 2008. Erythrophagocytosis by renal tubular cells. Kidney Int 74:398.

Muntner P, He J, Vupputuri S, Coresh J, Batuman V. 2003. Blood lead and chronic kidney disease in the general United States population: results from NHANES III. Kidney Int 63:1044-1050.

Navas-Acien A, Tellez-Plaza M, Guallar E, Muntner P, Silbergeld E, Jaar B, et al. 2009. Blood cadmium and lead and chronic kidney disease in us adults: A joint analysis. Am J Epidemiol 170:1156-1164.

Noh JY, Park JS, Lim KM, Kim K, Bae ON, Chung SM, et al. 2010. A naphthoquinone derivative can induce anemia through phosphatidylserine exposure-mediated erythrophagocytosis. J Pharmacol Exp Ther 333:414-420.

Otogawa K, Kinoshita K, Fujii H, Sakabe M, Shiga R, Nakatani K, et al. 2007. Erythrophagocytosis by liver macrophages (kupffer cells) promotes oxidative stress, inflammation, and fibrosis in a rabbit model of steatohepatitis: Implications for the pathogenesis of human nonalcoholic steatohepatitis. Am J Pathol 170:967-980.

Patra RC, Swarup D, Dwivedi SK. 2001. Antioxidant effects of alpha tocopherol, ascorbic acid and l-methionine on lead induced oxidative stress to the liver, kidney and brain in rats. Toxicology 162:81-88.

Rasmussen ML, Folsom AR, Catellier DJ, Tsai MY, Garg U, Eckfeldt JH. 2001. A prospective study of coronary heart disease and the hemochromatosis gene (hfe) c282y mutation: The atherosclerosis risk in communities (aric) study. Atherosclerosis 154:739-746.

Ryan MJ, Johnson G, Kirk J, Fuerstenberg SM, Zager RA, Torok-Storb B. 1994. Hk-2: An immortalized proximal tubule epithelial cell line from normal adult human kidney. Kidney Int 45:48-57.

Schutz A, Bergdahl IA, Ekholm A, Skerfving S. 1996. Measurement by icp-ms of lead in plasma and whole blood of lead workers and controls. Occup Environ Med 53:736-740.

Sheerin NS, Sacks SH, Fogazzi GB. 1999. In vitro erythrophagocytosis by renal tubular cells and tubular toxicity by haemoglobin and iron. Nephrol Dial Transplant 14:1391-1397.

Shettihalli AK, Gummadi SN. 2013. Biochemical evidence for lead and mercury induced transbilayer movement of phospholipids mediated by human phospholipid scramblase 1. Chem Res Toxicol 26:918-925.

Stacchiotti A, Morandini F, Bettoni F, Schena I, Lavazza A, Grigolato PG, et al. 2009. Stress proteins and oxidative damage in a renal derived cell line exposed to inorganic mercury and lead. Toxicology 264:215-224.

Thiebault C, Carriere M, Milgram S, Simon A, Avoscan L, Gouget B. 2007. Uranium induces apoptosis and is genotoxic to normal rat kidney (nrk-52e) proximal cells. Toxicol Sci 98:479-487.

Trump BF, Tisher CC, Saladino AJ. 1969. The neprhon in heath and disease. In: The biological basis of medicine, Vol. 6, (Bittar E, Bittar N, eds). London, New York:Academic Press Inc., 387-494.

Valko M, Morris H, Cronin MT. 2005. Metals, toxicity and oxidative stress. Curr Med Chem 12:1161-1208.

Vallon V, Thomson SC. 2012. Renal function in diabetic disease models: The tubular system in the pathophysiology of the diabetic kidney. Annu Rev Physiol 74:351-375.

Wang H, Nishiya K, Ito H, Hosokawa T, Hashimoto K, Moriki T. 2001. Iron deposition in renal biopsy specimens from patients with kidney diseases. Am J Kidney Dis 38:1038-1044.

Wang L, Wang H, Hu M, Cao J, Chen D, Liu Z. 2009. Oxidative stress and apoptotic changes in primary cultures of rat proximal tubular cells exposed to lead. Arch Toxicol 83:417-427.

Wang L, Li J, Li J, Liu Z. 2010. Effects of lead and/or cadmium on the oxidative damage of rat kidney cortex mitochondria. Biol Trace Elem Res 137:69-78.

Wang L, Wang H, Li J, Chen D, Liu Z. 2011. Simultaneous effects of lead and cadmium on primary cultures of rat proximal tubular cells: Interaction of apoptosis and oxidative stress. Arch Environ Contam Toxicol 61:500-511.

Willekens FL, Werre JM, Kruijt JK, Roerdinkholder-Stoelwinder B, Groenen-Dopp YA, van den Bos AG, et al. 2005. Liver kupffer cells rapidly remove red blood cell-derived vesicles from the circulation by scavenger receptors. Blood 105:2141-2145.

Zager RA, Johnson AC, Hanson SY, Wasse H. 2002. Parenteral iron formulations: A comparative toxicologic analysis and mechanisms of cell injury. Am J Kidney Dis 40:90-103.

Zager RA, Johnson AC, Hanson SY. 2004. Parenteral iron nephrotoxicity: Potential mechanisms and consequences. Kidney Int 66:144-156.

Zhao W, Chen SS, Chen Y, Ahokas RA, Sun Y. 2008. Kidney fibrosis in hypertensive rats: Role of oxidative stress. Am J Nephrol 28:548-554.

Figure Legends

Figure 1. Effects of Pb^{2+}-exposed erythrocytes on renal tubular epithelial cells. Freshly isolated human erythrocytes were exposed to Pb^{2+} (0, 10 and 20 μM) for 1 hr at 37°C, and co-incubated with HK-2 tubular epithelial cells for 24 hr. *(A)* Cell viability was measured in HK-2 cells with or without co-incubation of Pb^{2+}-exposed erythrocytes. *(B)* Interaction between Pb^{2+}-exposed erythrocytes and HK-2 cells was observed (red arrows). Bar = 20 μm. *(C)* Adherence of Pb^{2+}-exposed erythrocytes to HK-2 cells was examined using scanning electron microscopy. Bar = 5 μm. *(D)* HK-2 cells which were fluorescence-positive by engulfment of CFDA-loaded erythrocytes were analyzed in flow cytometry. Representative histograms and the number of positive HK-2 cells were presented. Values are the mean ± SEM of more than three independent experiments. * $p<0.05$ vs. corresponding control determined by one-way ANOVA followed by Duncan's multiple range test, # $p<0.05$ vs. HK-2 cells exposed to Pb^{2+} 20 μM in the absence of erythrocytes determined by Student's t-test.

Figure 2. Role of Pb^{2+}-induced erythrophagocytosis in renal tubular damage. *(A and B)* After erythrocytes were incubated with Pb^{2+} for 1 hr at 37°C, flow cytometric analysis was employed to determine externalization of phosphatidylserine (PS) in outer membrane *(A)* or generation of microvesicles (MV) from erythrocytes *(B)*. Representative histograms and quantified bar graphs were shown. *(C)* Pb^{2+}-induced erythrophagocytosis in HK-2 cells was reversed by the addition of purified annex V, which masked externalized PS in erythrocytes. *(D and E)* After co-incubation of HK-2 cells with Pb^{2+}-exposed erythrocytes for 4 hr at 37°C, renal tubular damage was determined. Generation of ROS was measured by DCF fluorescence in HK-2 cells using flow cytometry *(D)* and the change of mRNA level for nephrotoxic biomarkers (NGAL and KIM-1) in HK-2 cells were detected by qRT-PCR *(E)*. Data were subjected to one-way ANOVA followed by Duncan's multiple range test (A, B, D) or Student's t-test (C, E) to determine the statistical significance. Values are the mean ± SEM of more than three independent experiments. *$p<0.05$ vs. corresponding control.

Figure 3. Accumulation of iron in the spleen and kidney of rats exposed to lead *in vivo.* After rats were exposed to Pb^{2+}-contaminated drinking water (0, 250, and 1000 ppm of Pb^{2+}) for 12

weeks, the spleen and kidney were dissected and fixed for Prussian blue staining. Representative microscopic photographs of spleen *(A)* and kidney *(B)* from rats in each group were shown. Bar = 100 μm.

Figure 4. Renal damage in rats exposed to lead *in vivo*. Kidney tissue was isolated from the rats exposed to Pb^{2+} for 12 weeks, and renal damage associated with erythrophagocytosis was determined. *(A)* Generation of ROS in kidney was measured by DHE fluorescence. *(B)* Histopathological changes were evaluated by H&E staining. Representative photos were shown. Bar = 100 μm. Relative kidney weight *(C)* and the level of blood urea nitrogen (BUN) in serum *(D)* from rats exposed to Pb^{2+} were measured. *(E)* The change in mRNA level of NGAL and KIM-1 in kidney was detected by qRT-PCR. Data were subjected to one-way ANOVA followed by Duncan's multiple range test (E) or Student's t-test (C, D) to determine the statistical significance. Values are the mean ± SEM of six to nine rats/group. * $p<0.05$ vs. corresponding control.

Figure 5. Renal fibrosis following Pb^{2+} exposure. *(A and B)* After rats were exposed to Pb^{2+}-contaminated drinking water (0, 250, and 1000 ppm of Pb^{2+}) for 12 weeks, the kidney was isolated to examine renal fibrosis. *(A)* Fibrotic collagen deposition was examined by Masson trichrome staining (black arrows). Representative photos were shown. Bar = 100 μm. *(B)* The level of TGF-β mRNA in kidney was quantified by qRP-PCR. Values are the mean ± SEM of five rats/group. *(C)* After *in vitro* co-incubation of HK-2 cells with Pb^{2+}-exposed erythrocytes for 4 hr, the mRNA level of TGF-β in HK-2 cells was determined. Data were subjected to one-way ANOVA followed by Duncan's multiple range test. Values are the mean ± SEM of five experiments. * $p<0.05$ vs. corresponding control.

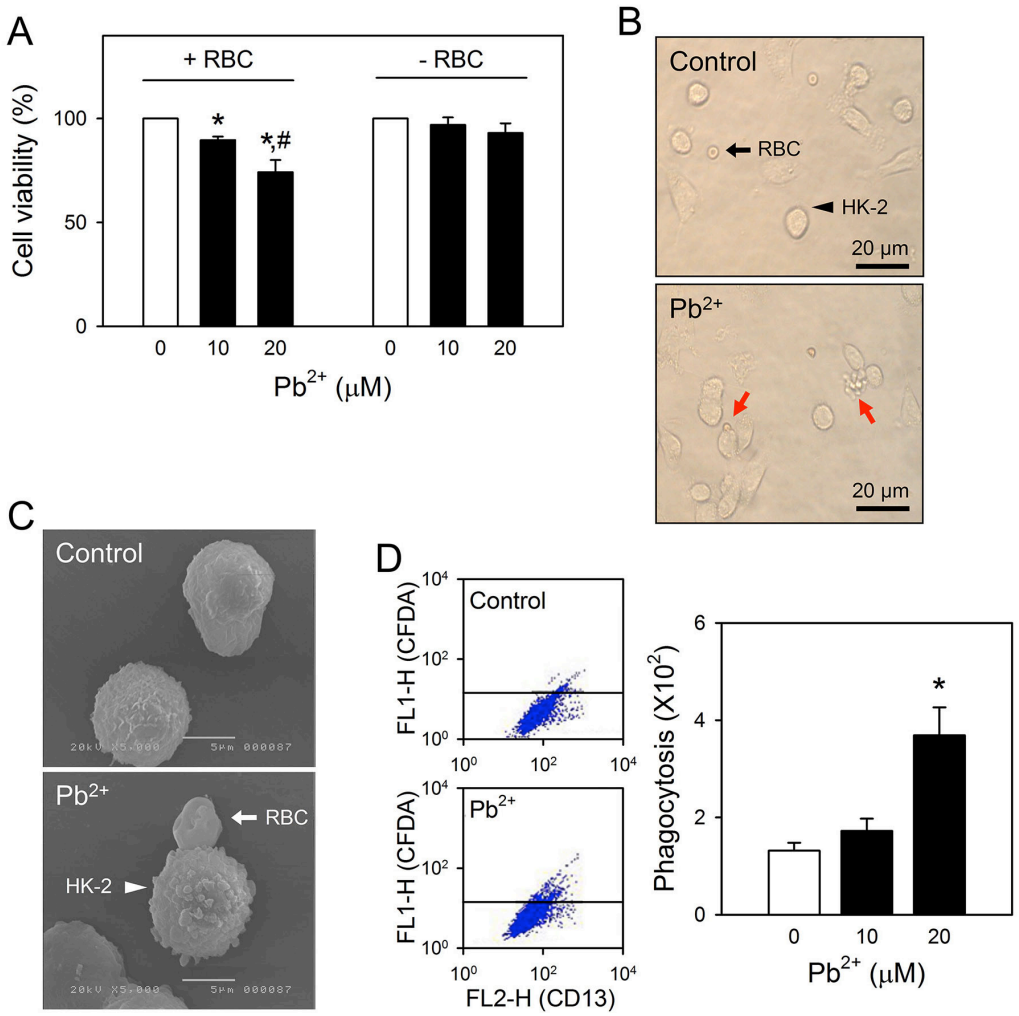
A
+ RBC
- RBC
Cell viability (%)
100
50
0
*
*,#
0
10
20
0
10
20
Pb2+ (μM)
B
Control
RBC
HK-2
20 μm
Pb2+
20 μm
C
Control
Pb2+
RBC
HK-2
D
Control
Pb2+
FL1-H (CFDA)
FL2-H (CD13)
Phagocytosis (X10^2)
6
4
2
0
*
0
10
20
Pb2+ (μM)

Figure 1

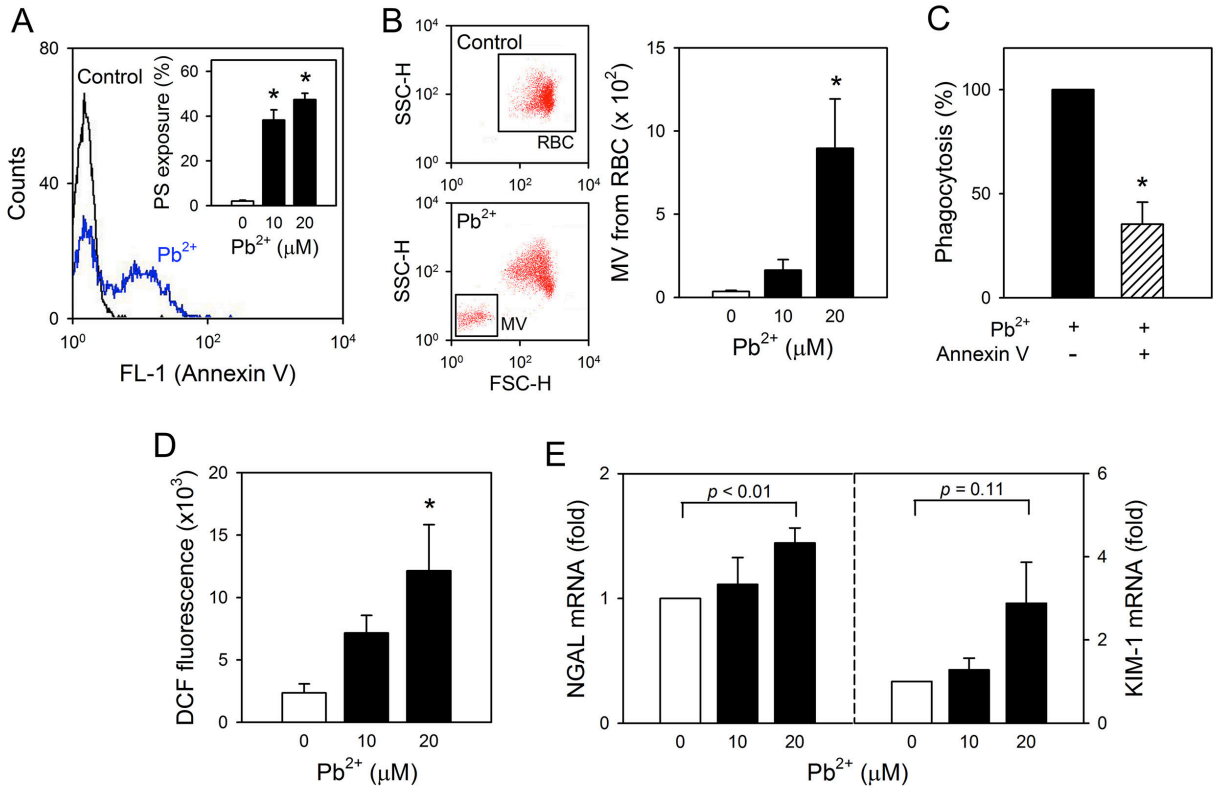
A
Control
Counts
FL-1 (Annexin V)
PS exposure (%)
Pb2+ (μM)
B
Control
RBC
SSC-H
FSC-H
MV
MV from RBC (x 10^2)
C
Phagocytosis (%)
Annexin V
D
DCF fluorescence (x10^3)
E
p < 0.01
p = 0.11
NGAL mRNA (fold)
KIM-1 mRNA (fold)

Figure 2

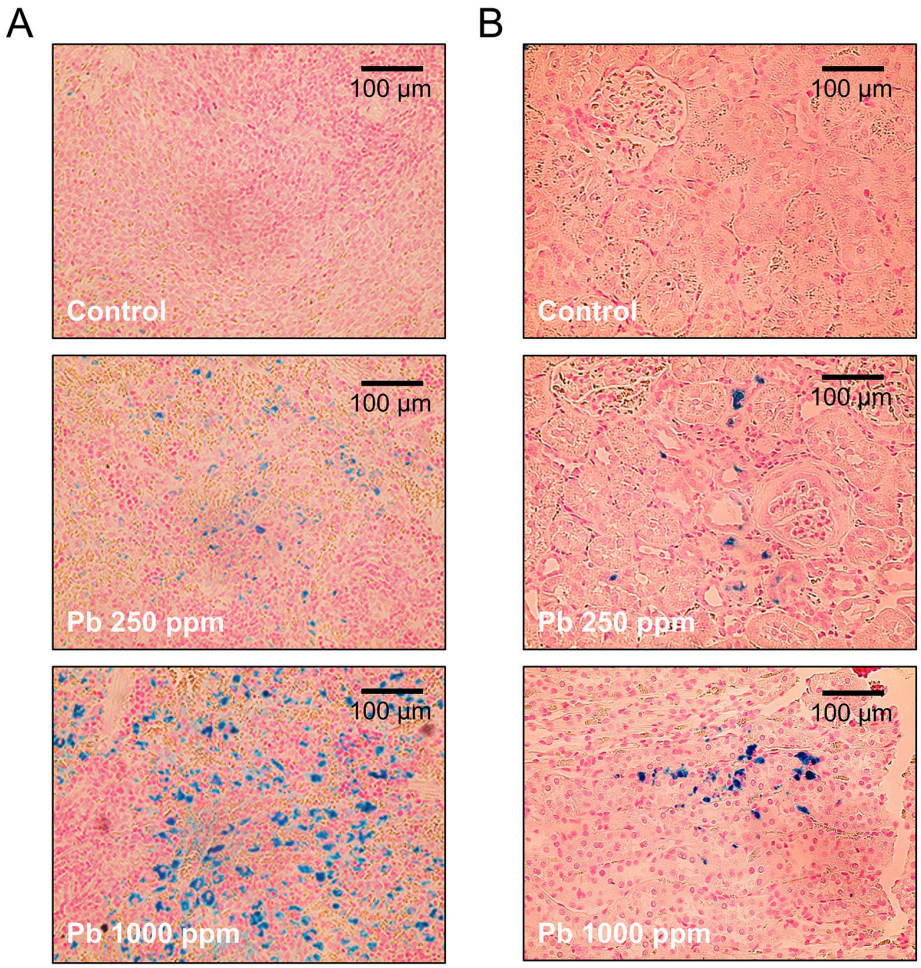
A
B
100 µm
Control
100 µm
Control
100 µm
Pb 250 ppm
100 µm
Pb 250 ppm
100 µm
Pb 1000 ppm
100 µm
Pb 1000 ppm

Figure 3

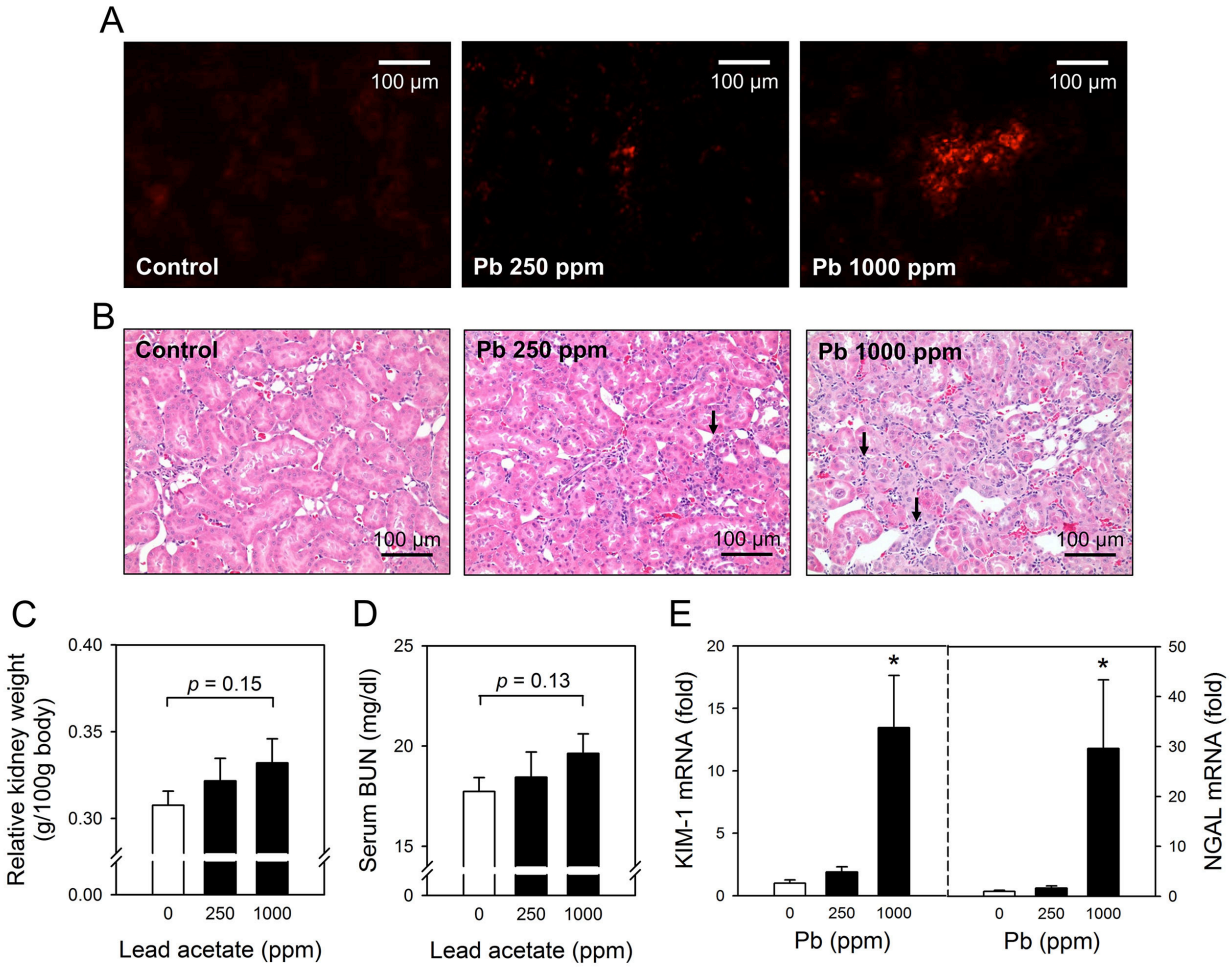
A
100 μm
Control
Pb 250 ppm
Pb 1000 ppm
B
Control
Pb 250 ppm
Pb 1000 ppm
100 μm
C
Relative kidney weight (g/100g body)
p = 0.15
Lead acetate (ppm)
D
Serum BUN (mg/dl)
p = 0.13
Lead acetate (ppm)
E
KIM-1 mRNA (fold)
NGAL mRNA (fold)
Pb (ppm)
Pb (ppm)

Figure 4

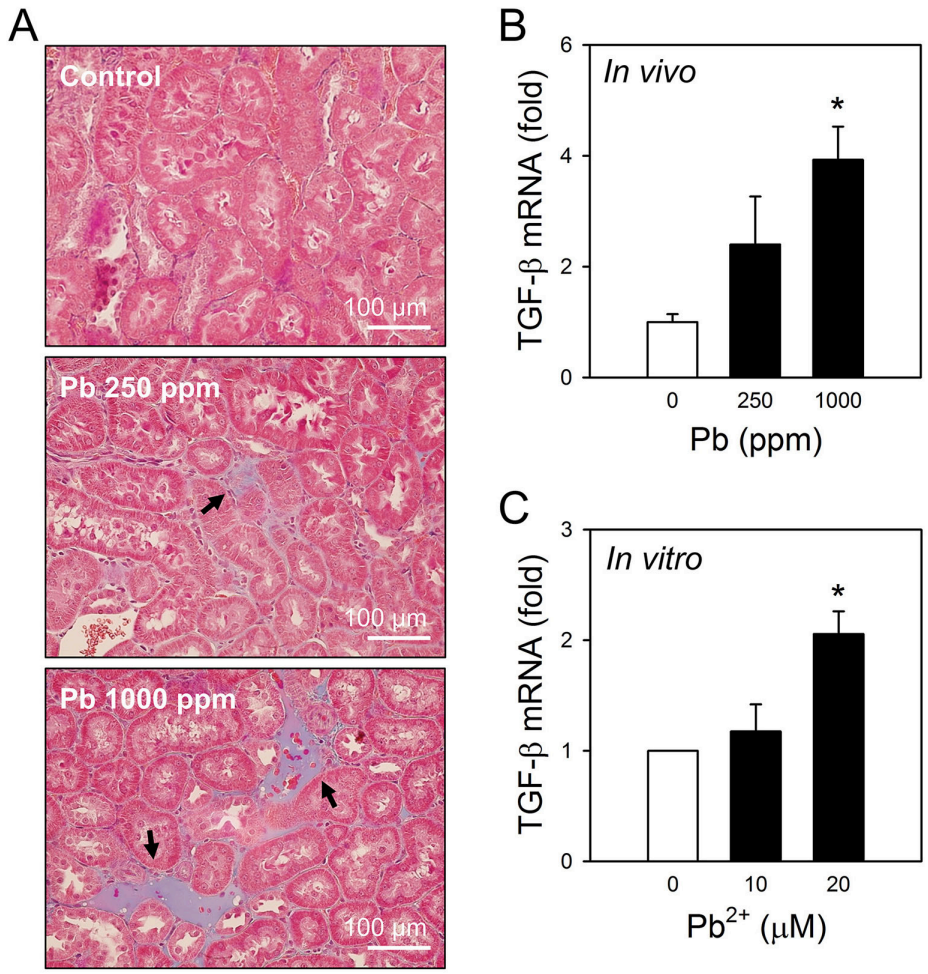
A
Control
100 μm
Pb 250 ppm
100 μm
Pb 1000 ppm
100 μm
B
In vivo
TGF-β mRNA (fold)
0
2
4
6
*
0
250
1000
Pb (ppm)
C
In vitro
TGF-β mRNA (fold)
0
1
2
3
*
0
10
20
Pb2+ (μM)

Figure 5